Available online at www.sciencedirect.com

ScienceDirect

Nuclear Physics B (Proc. Suppl.) 243–244 (2013) 12–24

NUCLEAR PHYSICS B PROCEEDINGS SUPPLEMENTS

www.elsevier.com/locate/npbps

The Alpha Magnetic Spectrometer on the International Space Station

Samuel Ting[a]

[a] *MIT, Boston, US and Cern, Geneva, Switzerland*

Abstract

The Alpha Magnetic Spectrometer is a precision, large acceptance particle physics detector which was deployed on the International Space Station (ISS) in May 2011. It will be on the ISS for the entire lifetime of the Space Station of about 20 years. To date, the detector has collected over 24 billion cosmic ray events. Among the physics objectives of AMS are the search for an understanding of Dark Matter, Antimatter and the origin of cosmic rays as well as the exploration of new physics phenomena. This report presents an overview of the operations and performance of the AMS experiment on the ISS as well as the progress of the analysis of the data collected over one year of operations in space.

Keywords: International Space Station, Cosmic Rays, antimatter, dark matter.

The Alpha Magnetic Spectrometer (AMS) is a U.S. Department of Energy sponsored experiment deployed on the International Space Station for a long duration mission (10-20 years) searching for an understanding of the origin of Dark Matter, the existence of Antimatter, the origin and properties of cosmic rays and to explore new phenomena from the venue of space [1]. Figure 1 shows the AMS Detector as installed as an external payload of the Space Station.

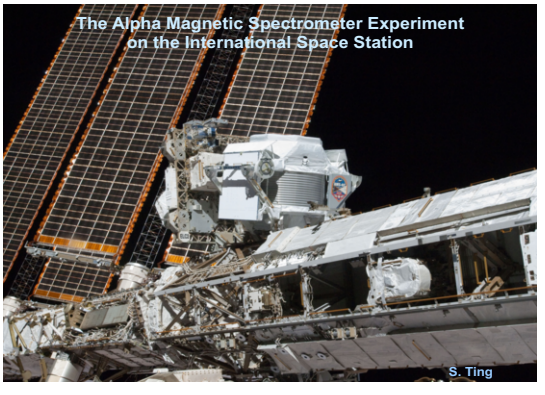

Fig. 1. AMS was delivered and installed on the ISS in May 2011.

As shown in Figure 2, AMS is a precision multipurpose spectrometer composed of an array of particle physics detectors to measure the charge (Z), energy (E~P) of particles and nuclei and a permanent magnet to measure the momentum [2].

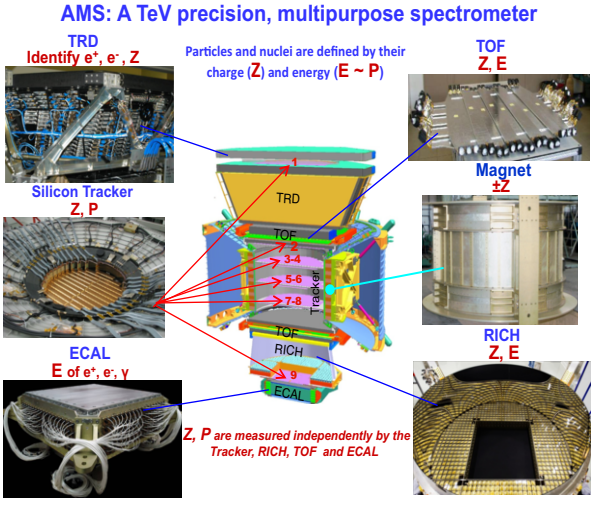

Fig. 2. The AMS Detector is made up of a central permanent magnet surrounded by an array of precision particle detectors.

http://dx.doi.org/10.1016/j.nuclphysbps.2013.09.028

Charge and energy are measured independently by the Tracker, Ring Image Cerenkov Counter (RICH), Time of Flight counters (TOF) and Electromagnetic Calorimeter (ECAL). The Transition Radiation Detector (TRD) identifies electrons and positrons by transition radiation and measures their charge and identifies nuclei by dE/dX. As seen in Figure 3, the Magnet and the Veto System (ACC) reject random cosmic rays. The ACC has a measured efficiency of better than 0.99999. The AMS magnet was previously flown in the AMS-01 mission onboard space shuttle Discovery in 1998 [3]. Over the 12 years between the AMS-01 mission (1998) and AMS-02 (measured in 2010), the field remained the same (to <1%).

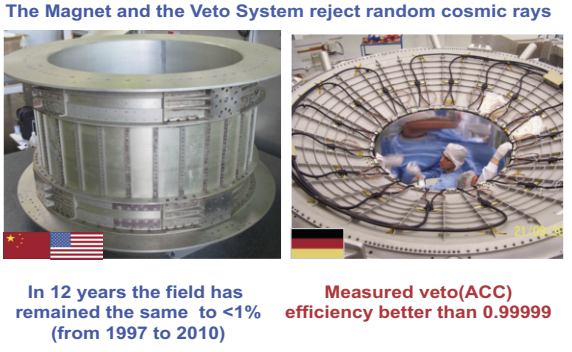

Fig. 3. The Ams Magnet and the Veto System (ACC) reject random cosmic rays.

The AMS Detector provides a sensitive search for Antimatter with Helium/antiHelium > 10^{10}. As shown in Figure 4, this is accomplished by:

a) using minimal material in the detector so that the detector itself does not become a source of large angle scattering, and
b) conducting repetitive measurements of momentum to ensure that particles which had large angle scattering are not confused with the signal, and by multiple independent measurements of the Charge (|Z|) as shown in Figure 5.

The AMS Detector also provides a sensitive search for the origin of Dark Matter with $p/e^+ > 10^6$.
As shown in Figure 6, this is accomplished by:

a) using minimal material in the TRD and TOF so that the detector does not become a source of e^+,
b) using a magnet to separate the TRD and ECAL so that e+ produced in the TRD will be swept away and not enter ECAL. In this way, the rejection power of TRD and ECAL are independent,
c) matching momentum of 9 tracker planes with ECAL energy measurements.

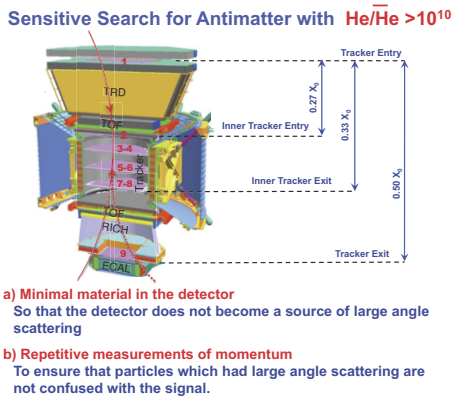

Fig. 4. High sensitivity search for antimatter is a goal of AMS.

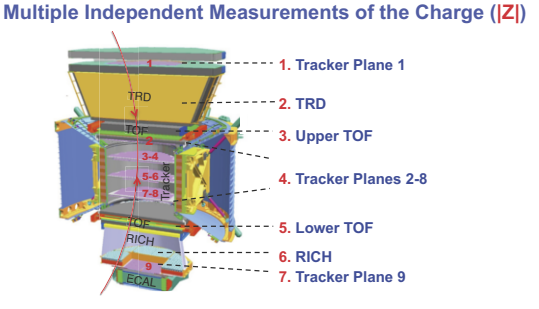

Fig. 5. Multiple independent measurements of the charge of passing particles.

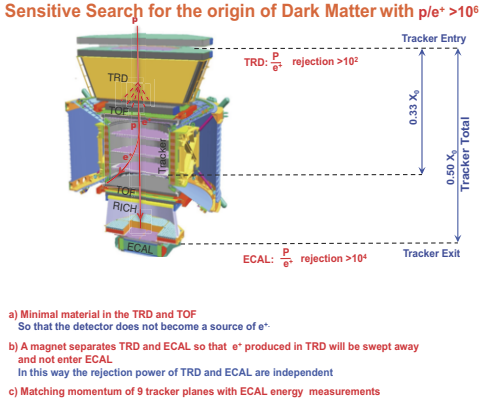

Fig. 6. High sensitivity search for Dark Matter is a goal of AMS.

The AMS Detector was built in AMS collaborating universities and institutes around the world and shipped to CERN-Geneva for assembly, testing and space qualification testing. CERN provided two test beam calibrations of the AMS Detector simulating the detector's performance with high-energy particles in space. Figure 7 illustrates a sample of the major results from the beam testing in 2010. After thermal vacuum and electromagnetic interference testing at ESTEC (European Space Agency Test Center) in the Netherlands, AMS returned to CERN and was flown to Kennedy Space Center for final tests and prelaunch processing. On May 16, 2011 at 8:56AM, AMS was launched to the International Space Station as the prime payload onboard space shuttle Endeavour (see Figure 8). AMS was successfully deployed on the S-3 truss of the U.S. ISS National Laboratory (see Figure 9) on May 19th at 5:15AM and at 9:35AM, AMS began taking data.

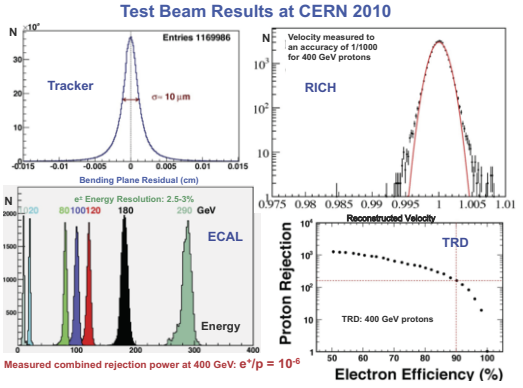

Fig. 7. Major results from the AMS test beam calibration at CERN (2010)

Figure 8: The launch of space shuttle Endeavour on May 16, 2011. The 7.5 ton AMS Detector was the primary payload in the shuttle cargo bay.

Figure 9: AMS was successfully installed on the ISS on May 19, 2011 and began taking data about four hours later

AMS operations in space are based around the data flow between the AMS detector and the AMS Payload Operations and Control Center (POCC) and Science Operations Center (SOC), located at CERN-Geneva. At an average rate of 10 Mbit/s, data from AMS is transmitted over the High Rate Data Link (HRDL) on the ISS. Using the Ku radiofrequency band (Ku band), it is bounced off one of the geosynchronous Tracking and Data Relay Satellites (TDRS) and down to the White Sands Ground Terminal in New Mexico. From there it is directed over NASA networks to dedicated DOE computers located within the Payload Operations and Integration Center (POIC) at Marshall Space Flight Center (MSFC) where it is written on disk and copied to the POCC. Commands from the POCC follow this path in reverse over the Low Rate Data Link (LRDL) using the S-band. Both a complete and immediate stream of monitoring data (temperatures, voltages, etc.) at 30 Kbit/s each are also sent from AMS. Located in the crew quarters onboard the ISS is the dedicated AMS Laptop which records and stores all AMS data for up to two months. This data is recovered later whenever there is a dropout anywhere along the chain. This flow of data is depicted in Figure 10.

As noted in Figure 11, the thermal control of AMS is the most challenging task in the operation of AMS in space. The thermal environment on the ISS is constantly changing due to solar beta angle (β, the angle between the ISS orbital plane and the solar vector as illustrated in Figure 12), the changing position of the ISS radiators and solar arrays and the ISS attitude that changes primarily for visiting

vehicles (as shown in Figures 13 and 14). AMS contains over 1,100 temperature sensors and 298 heaters which are monitored around the clock in the AMS POCC to assure that the components stay within their strict thermal limits and avoid permanent damage.

Figure 10: AMS Operations: The flow of data from AMS to the Payload Operations Control Center (POCC) and the flow of commands from the POCC to AMS.

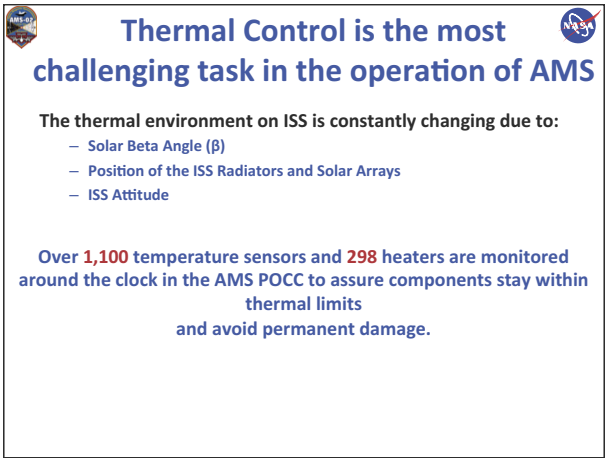

Figure 11: The thermal environment of AMS changes dramatically as the ISS orbits the Earth every 90 minutes. The Thermal Control of AMS is critical and is the most challenging task in operating an experiment in space.

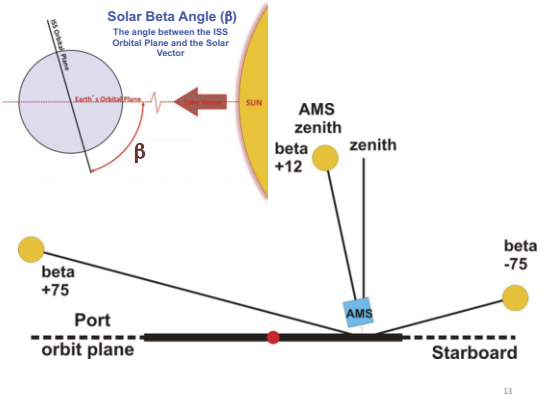

Figure 12: The solar beta angle is the angle between the ISS Orbital Plane and the Solar Vector.

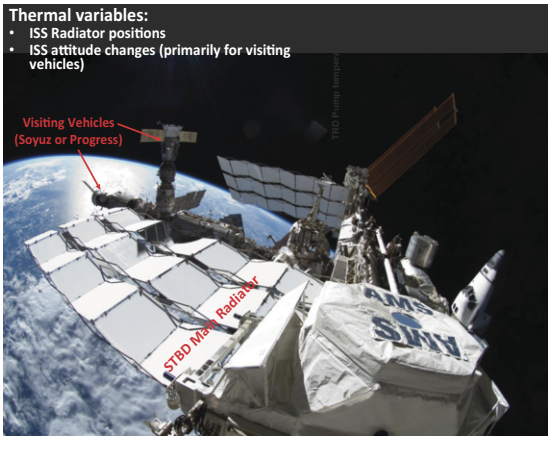

Figure 13: ISS radiator positions and ISS attitude changes (primarily as a result of visiting space vehicles) change the thermal conditions to which AMS is exposed.

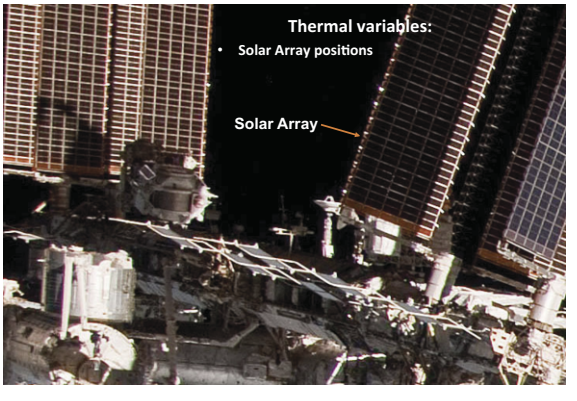

Figure 14: The ISS solar arrays are constantly changing position either casting shadows on AMS or exposing AMS to the direct sun thereby causing extreme thermal variations.

As shown in Figure 15, the TRD contains 24 heaters, 8 pressure sensors and 482 temperature sensors, the Tracker contains 4 pressure sensors, 32 heaters and 142 temperature sensors, the ECAL contains 80 temperature sensors, the TOF and ACC contain 64 temperature sensors, the magnet contains 68 temperature sensors and the RICH contains 96 temperature sensors all controlled by a system of computers that relay this vital information to the POCC and enables and disables the heaters from the POCC .

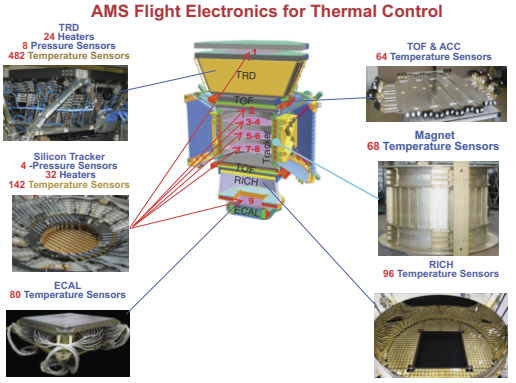

Figure 15: AMS Thermal System contains of 1,100 temperature sensors and 298 heaters.

Only the Tracker and TRD have their own dedicated thermal control systems. The control of the other detectors is done by the Global Thermal Control System.

To read out the 300,000 channels at up to 2 KHz, we developed a large set of computers (650) which are programmable from the POCC and which read out all the different detectors with up to 400% redundancy. Hundreds of these computers are interconnected in a tree like structure with a 100 Mbit/s serial link.

This complex system can be illustrated as follows.

As shown in Figures 16 and 17, the TRD [4] contain 5,248 pulse height channels which are read out via 24 Data Reduction computers (UDR) for analog to digital conversion, data reduction, formatting and sending to the next level and 4 Readout Computers (JINF-U) for collecting data from the UDRs, formatting and sending to the next level, control of 112 high and low voltage, distributing commands to UDR, combining busy signals and distributing trigger. Figures 18 and 19 show the TRD gas Control System. The TRD gas circuit layout (5 kg of CO_2 and 49 kg of Xe) is also controlled by the electronics (2 TRD Gas Control Computers – UCSCM) to ensure the readout of the 482 temperatures and 8 pressure sensors, to control the heaters, pumps and valves to keep the gas gain uniform and keep the TRD functioning. The leak rate of 5 μg/s caused by CO_2 diffusion corresponds to a lifetime of approximately 20 years in space.

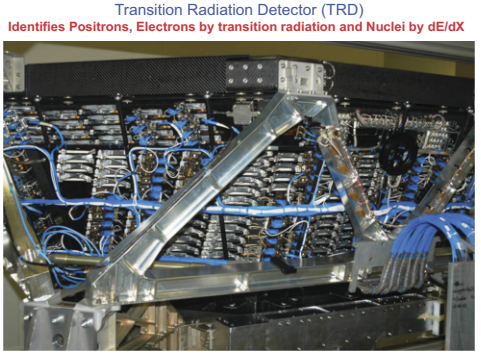

Figure 16: The TRD identifies positrons and electrons by transition radiation and nuclei by dE/dX.

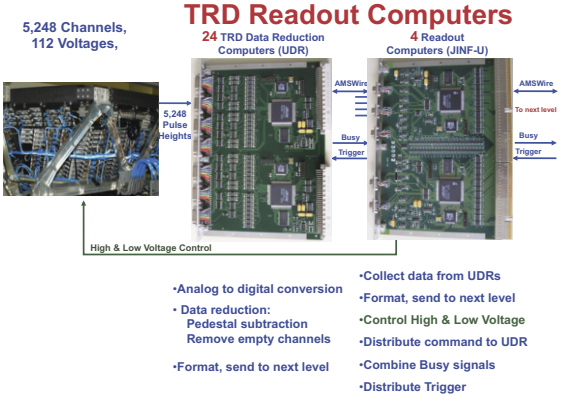

Figure 17: The TRD Data Reduction and Readout Computers.

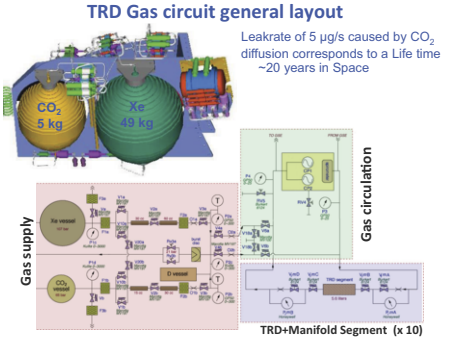

Figure 18: The control circuit of the TRD Gas system which circulates 5 kg of CO_2 and 49 kg of Xe.

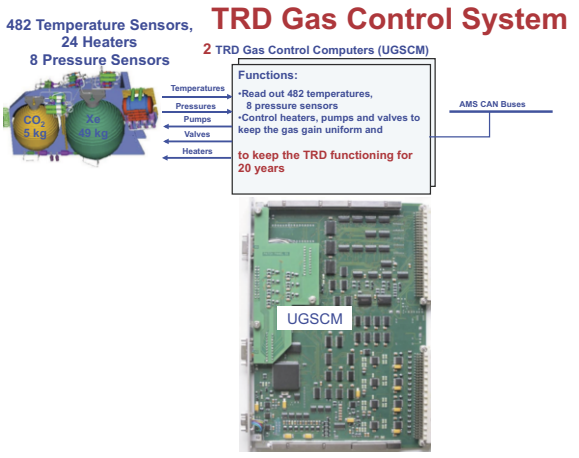

Figure 19: The TRD Gas Control Computers enable the TRD to operate for 20 years.

Figure 20 shows the TRD performance on ISS. As seen, the proton rejection for TRD at 90% e^+ efficiency is > 10^2 in the rigidity region < 600 GV.

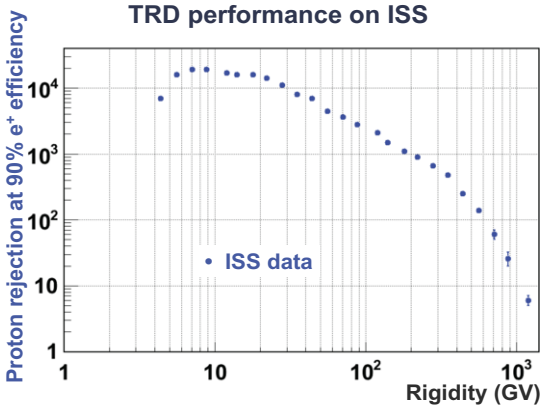

Figure 20: TRD performance in space at 90% e+ efficiency.

The Time of Flight System [5] consists of two TOF counter systems installed in the upper and lower portions of the detector to measure velocity and charge of particles. The Time of Flight System is illustrated in Figure 21. As seen, it distinguishes different nuclei with dE/dX and provides time resolution of 80 ps at Z = 2 and 48 ps at Z = 6.

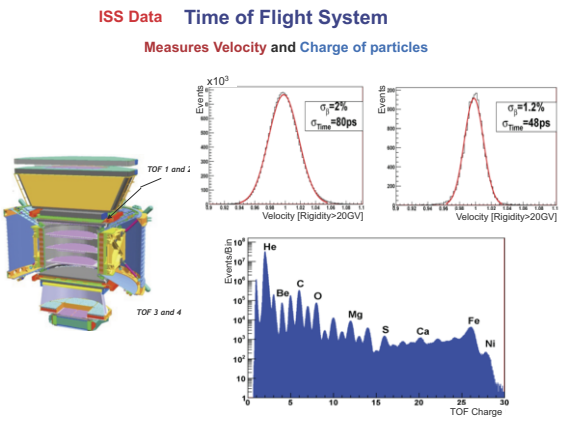

Figure 21: The Time of Flight System.

The Silicon Tracker [6] has a coordinate resolution of 10 μ and identifies nuclei by deE/dX. Figure 22 shows the tracker structure and test beam data. The nine tracker planes have excellent alignment stability. Figure 23 shows the alignment stability of 3 microns of the uppermost Tracker plane over 5 months. The Tracker contain 196,608 pulse height channels which read out via 192 Tracker Data Reduction (TDR) computers for analog to digital conversion, data reduction, formatting and sending to the next level and 16 Readout Computers (JINF-T) for collecting data from TDR, formatting and sending to the next level, controlling the 216 low voltages, combining busy signals, distribute Trigger and distribute commands to TDR. These computers are shown in Figure 24.

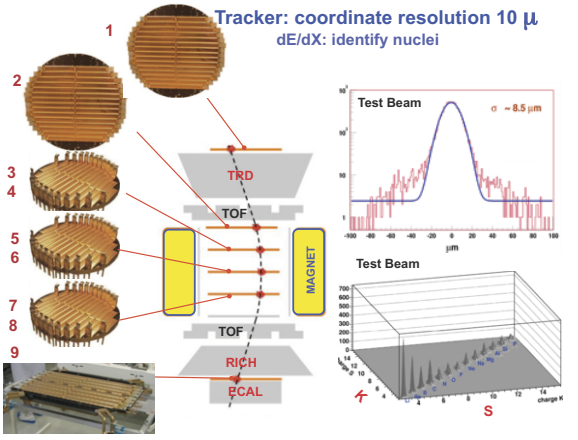

Figure 22: The location of the 9 Tracker planes and test beam data.

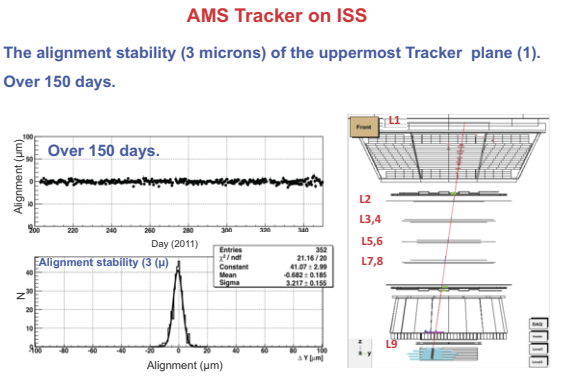

Figure 23: Alignment stability of the uppermost tracker plane over 5 months.

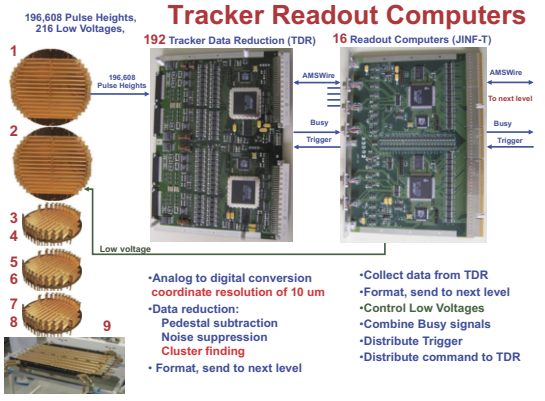

Figure 24: The Tracker Data Reduction and Readout Computers.

The Tracker Thermal Control System (TTCS) is operating flawlessly in space. The TTCS is a two-phase system which exchanges gas and liquid coming from the Tracker via the Heat Exchanger to a Condenser converting the gas back to its liquid phase. The CO_2 is then delivered by accumulator and pumped back into the Tracker to maintain the temperature to approximately 10^o C. This routing is shown in Figure 25. The TTCS is controlled by 2 Tracker Thermal Control Computers (TTEC) which readout the 142 temperatures and 4 pressure sensors shown in Figure 26. In reverse, the TTEC also controls the 32 heaters and pumps to keep the tracker temperature constant to 1 degree C. AMS has maintained excellent temperature stability over time as exemplified in Figure 27.

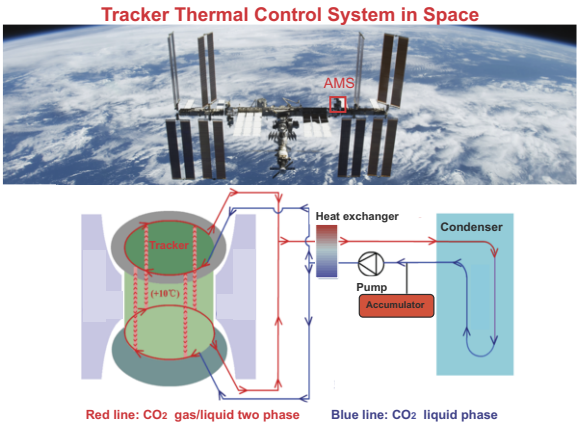

Figure 25: The Tracker Thermal Control System.

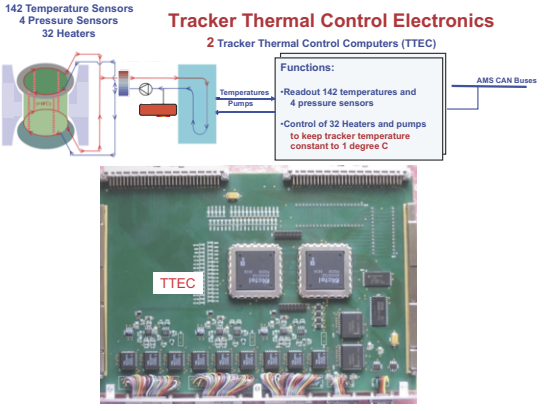

Figure 26: The control electronics for the Tracker Thermal Control System has the function of reading out the 142 thermostats and 4 pressure sensors and maintaining a constant temperature within 1 degree C.

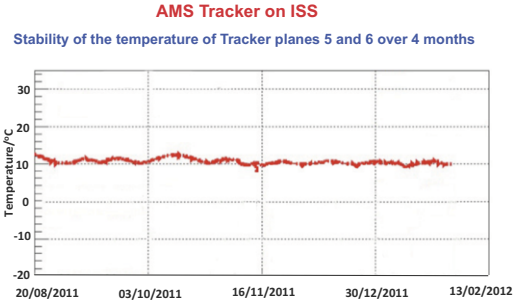

Figure 27: Temperature stability of Tracker Planes 5 and 6 over 4 months.

The Ring Image Cerenkov Counter (RICH) [7] contains 10,880 photosensors and 21,760 Signal Pulses to identify nuclei and their energy. Figure 28 shows the RICH and a sample event displaying the characteristic ring shape. The radius of the ring shows that the nuclei all have rigidity of 160 GV. The intensity of the ring differentiates different nuclei. Figure 29 presents a clean event penetrating the AMS upper Tracker, TRD, upper TOF, inner Tracker, Lower Time of Flight, RICH and lower Tracker. Figure 30 presents an event as seen by the RICH followed by the signal of a nuclei in the TeV range detected by the RICH in Figure 31.

The Electromagnetic Calorimeter [8] is shown in Figure 32. It is made up of 50,000 optical fibers distributed uniformly inside 600 kg of lead in 9 superlayers to provide 3D measurement of shower shape in 17 Xo to measure energy (3% resolution) of electrons and gamma rays up to 1 TeV. The data from ISS E-Cal proton rejection is shown in Figure 33.

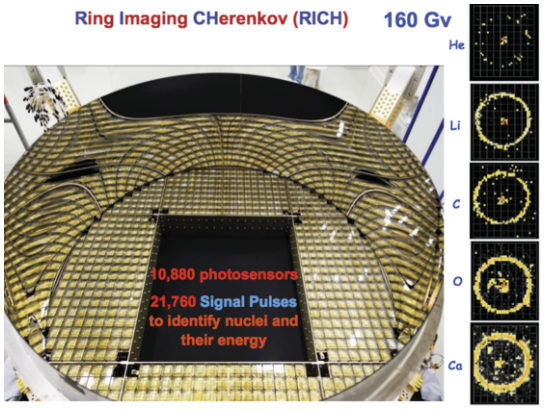

Figure 28: The Ring Image Cerenkov counter identifies nuclei and their energies.

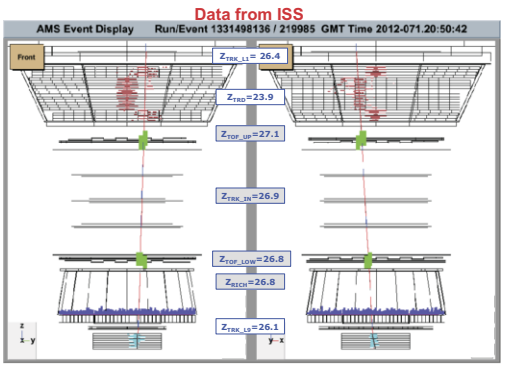

Figure 29: A signal of an event traversing the AMS Detector and reported energies by each detector.

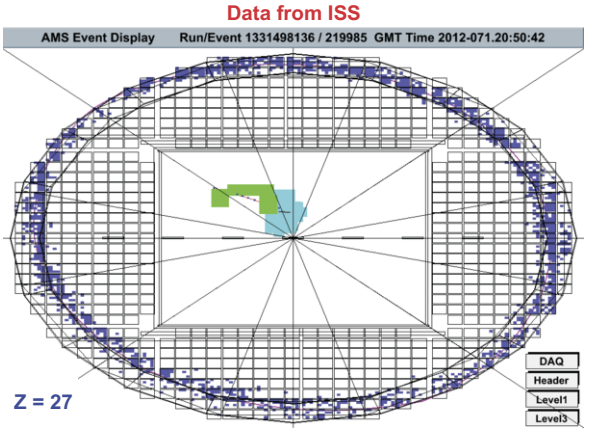

Figure 30: A signal of an event recorded by the RICH.

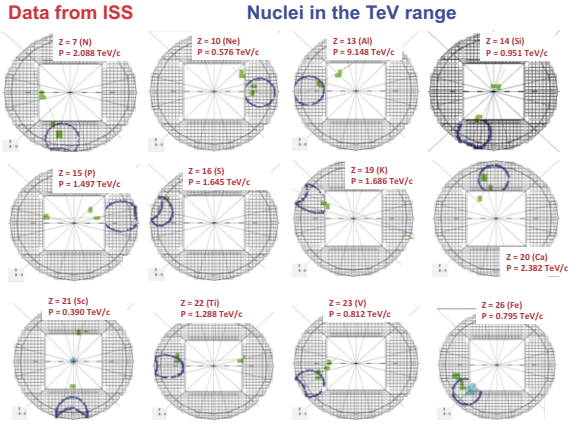

Figure 31: Nuclei in the TeV range.

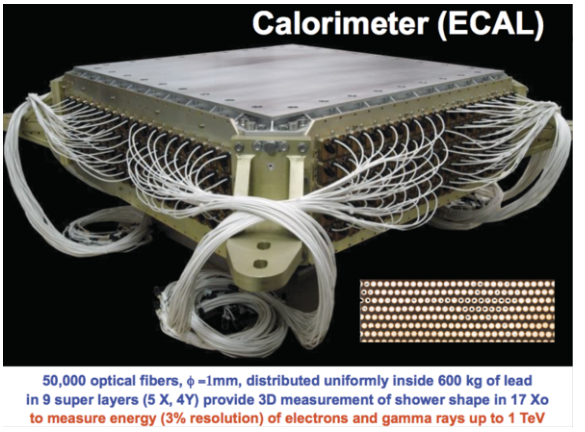

Figure 32: The AMS Electromagnetic Calorimeter measures energy of electrons and gamma rays up to 1 TeV.

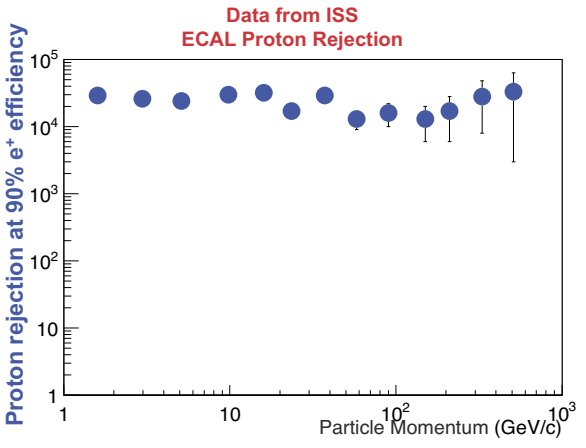

Figure 33: E-Cal proton rejection data from the ISS at 90% e^+ efficiency.

The AMS detectors, Data Acquisition and Thermal Systems have all functioned as designed. In the first 18 months of operations in space, AMS has collected over 24 billion events. Every year AMS will collect 16 billion events.

Among the physics objectives of AMS is the search for the origin of Dark Matter (Figure 34). The collision of cosmic rays produce e^+. Collisions of Dark Matter will produce additional e^+. The characteristics of this excess of e^+ can be measured very accurately by AMS.

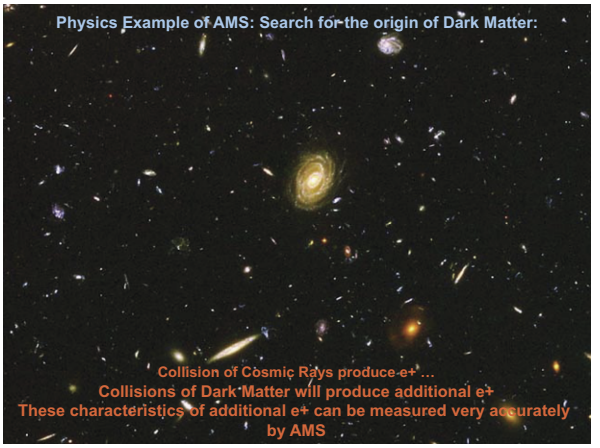

Figure 34: The characteristic excess of e+ can be accurately measured by AMS

Figures 35 through 39 present AMS data from the ISS.

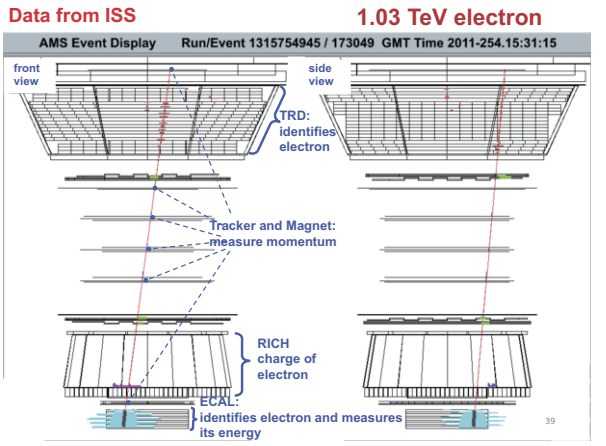

Figure 35: 1.03 TeV electron recorded by AMS.

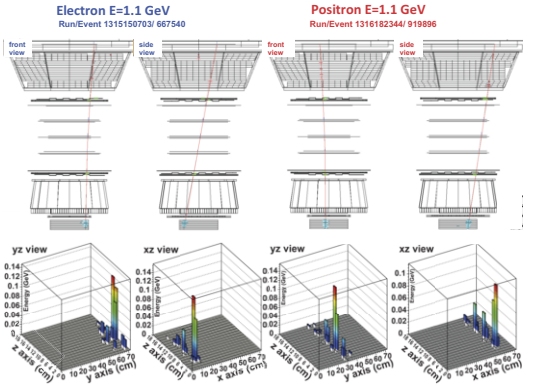

Figure 36: 1.1 GeV electron and 1.1 GeV positron recorded by AMS

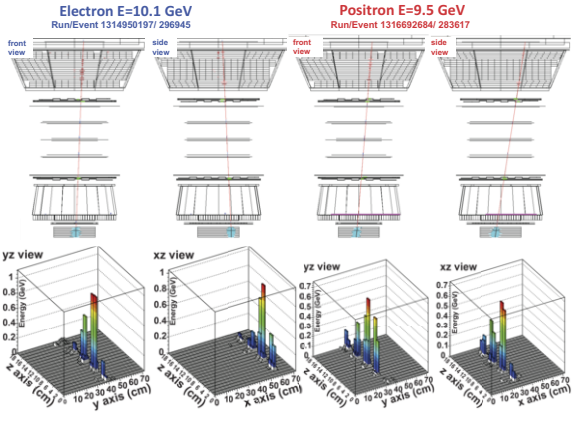

Figure 37: 10.1 GeV electron and 9.5 GeV positron recorded by AMS.

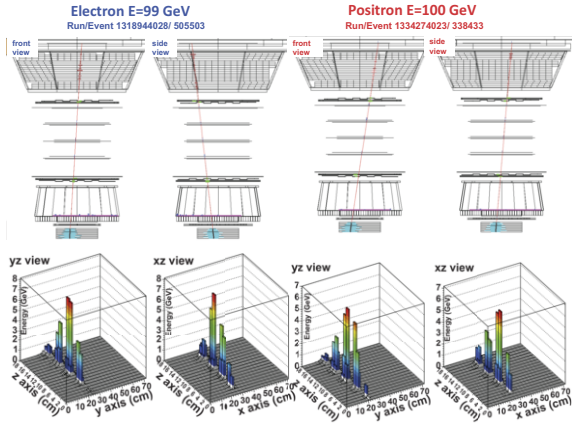

Figure 38: 99 GeV electron and 100 GeV positron recorded by AMS.

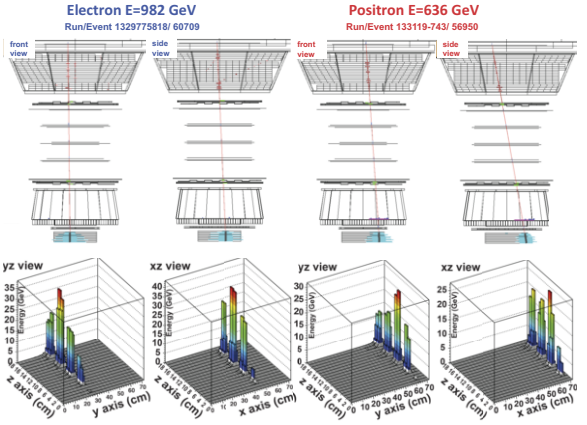

Figure 39: 982 GeV electron and 636 GeV positron recorded by AMS.

Our first publication will be on the $e^+/(e^++e^-)$ ratio over the $e^\pm$ energy range from 0.5 GeV to 350 GeV to an accuracy of 1 to 2%. The $e^+/(e^++e^-)$ ratio is a sensitive indicator of neutralinos as a candidate of dark matter. Subsequently, we will extend this measurement to 400, 500 GeV,… when there are enough statistics.

In the energy range between 65 to 100 GeV, we have 1,600 background free positron events. Figure 40 shows a comparison of recent experiments.

In addition to Dark Matter, one of the main objectives of AMS is the search for Antimatter (see Figure 41).

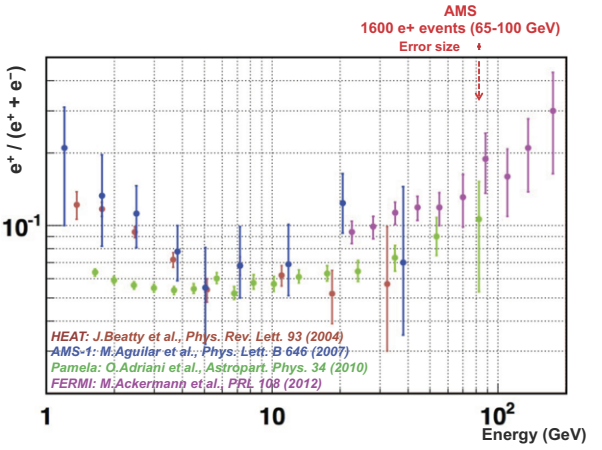

Figure 40: Data from recent experiments. Note AMS error size for 1600 e^+ events (65-100 GeV).

Unlike experiments which are searching for Antimatter through indirect means, AMS is distinct in its direct search for Antimatter through increased sensitivity (x 10^3 – 10^6 and increase in energy to ~TeV.

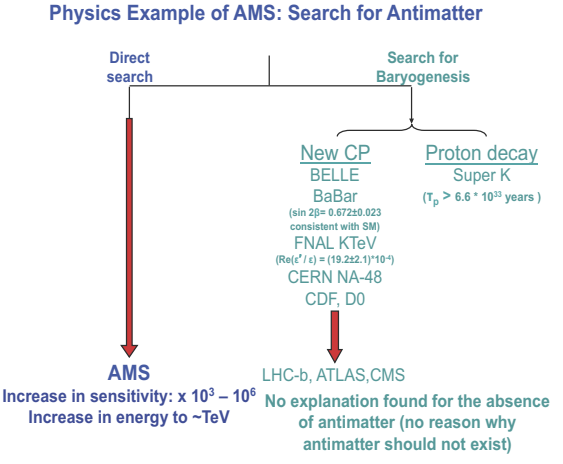

Figure 41: No explanation has been found for the absence of antimatter so there is no reason why antimatter should not exist. AMS is conducting a direct search for Antimatter from original sources in space.

To search for Antimatter nuclei, one must ensure the detector is capable of detecting all nuclei. Figure 42 shows the AMS measurement of nuclei on the ISS covering the elements in the Periodic Table.

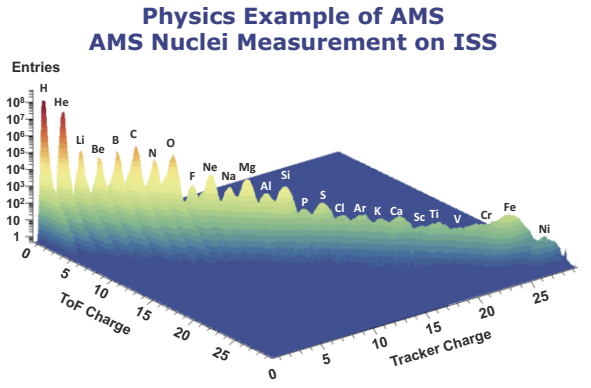

Figure 42: AMS nuclei measurement on the ISS.

The search for new phenomena is also a main objective of the AMS Experiment. As an example, AMS will continue its search for "Strangelets" begun during AMS-01. If there is material in the universe made up of u, d, and s quarks, then AMS will be able to detect it and definitively answer the question why is all material on Earth made only out of u and d quarks only. "Strangelets" are described in Figure 43.

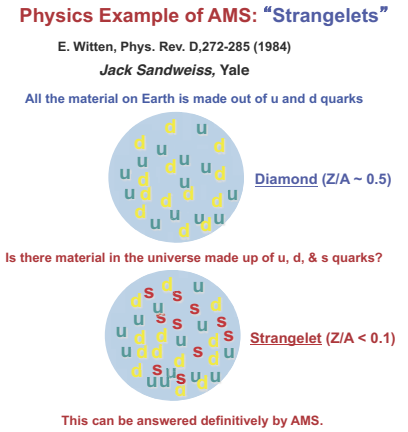

Figure 43: The study of "Strangelets" is one of the objectives of AMS.

Other examples of ongoing studies include the following.

- Boron/Carbon ratio up to TeV. As shown in Figure 44, the precise measurement of the energy spectra of B/C provides information on Cosmic Ray interactions and propagation as well as interactions with interstellar medium.

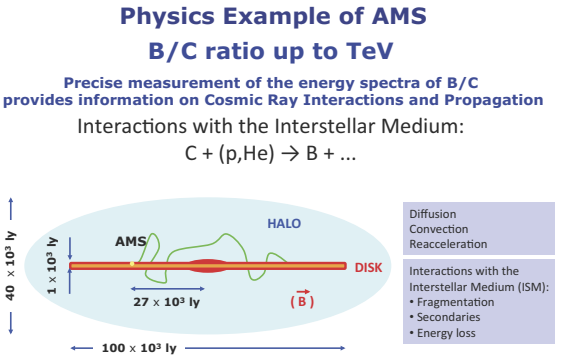

Figure 44: Boron to Carbon ratio up to TeV region is studied by AMS.

AMS measures the charge of Carbon in multiple independent measurements as seen in Figure 45. Figures 46 to 51 include measurements of Boron and Carbon at various rigidities.

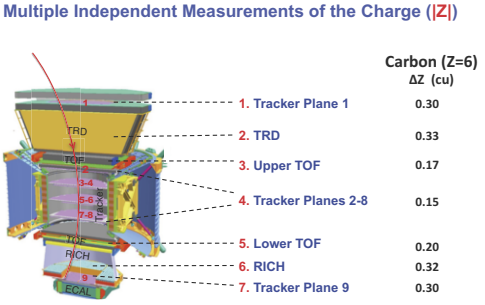

Figure 45: Multiple independent measurements of the Charge (|Z|) for Carbon.

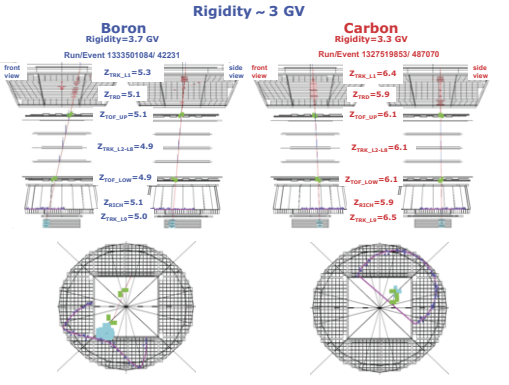

Figure 46: Boron to Carbon with Rigidity ~3 GeV.

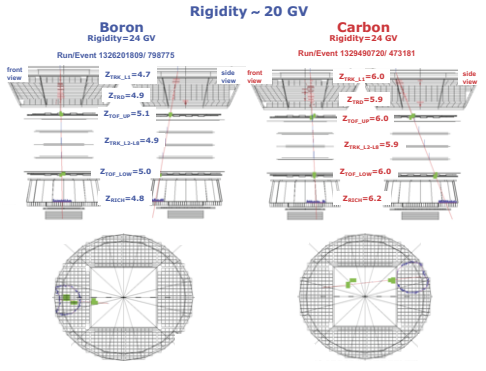

Figure 47: Boron to Carbon with rigidity of ~20 GeV.

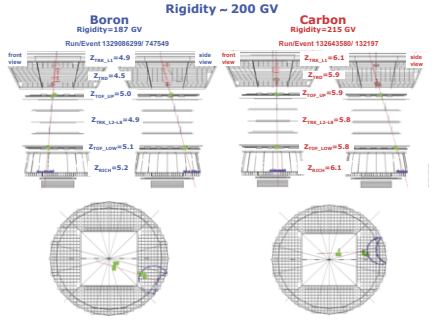

Figure 48: Boron to Carbon with Rigidity ~ 200 GeV.

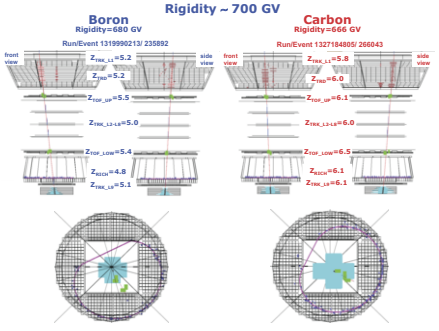

Figure 49: Boron to Carbon with Rigidity ~ 700 GeV.

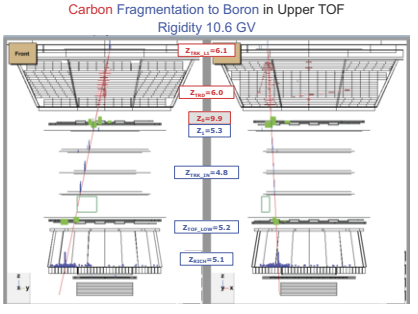

Figure 50: Carbon Fragmentation to Boron observed in the Upper Time of Flight with Rigidity of 10.6 GeV.

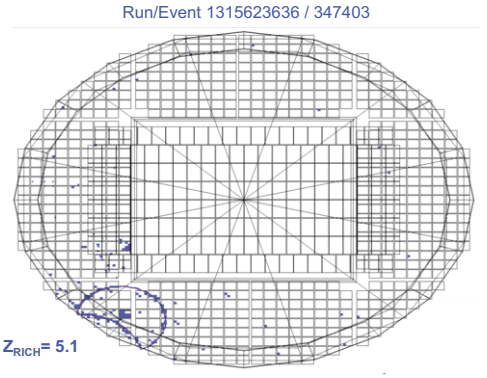

Figure 51: Boron to Carbon as observed in the RICH.

AMS is also studying particle yield. Figures 52 and 53 present examples of the He rate as a function of events/sec/GV and Rigidity.

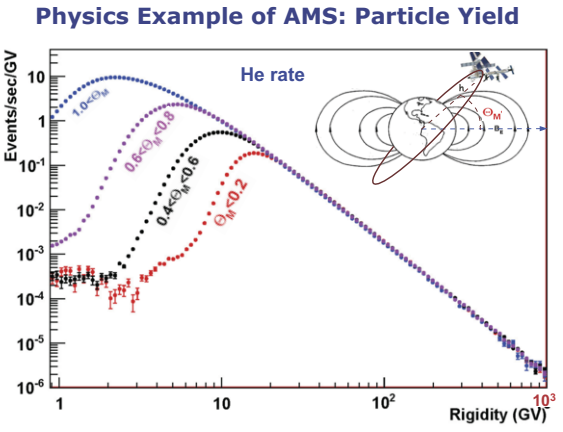

Figure 52: Example of particle yield: He rate from AMS

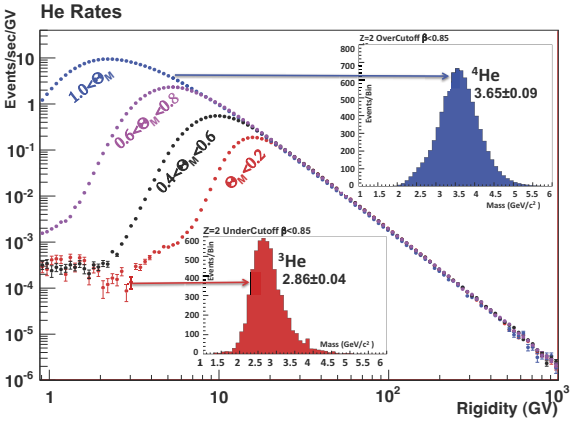

Figure 53: Example of particle yield: ^{3}He and ^{4}He rates from AMS.

To summarize, as noted in Figure 54, there are two kinds of cosmic rays traveling through space: Neutral cosmic rays (which have been measured for over 50 years) and Charged cosmic rays. Following experiments with balloons and satellites, AMS, using a magnetic spectrometer, is providing precision, long duration (10-20 years) measurement of high energy charged cosmic rays.

The ISS is an ideal platform for fundamental research and the study of charged cosmic rays from original sources in space. Indeed, the Cosmos is the ultimate laboratory, as seen in Figure 55, for the exploration of new physics and astrophysics phenomena.

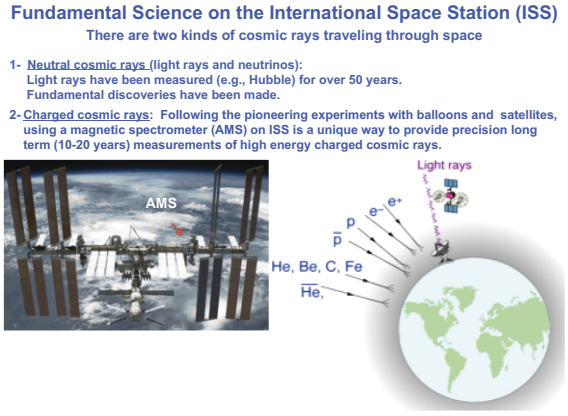

Figura 54: Two kinds of Cosmic rays traveling through space: Neutral and Charged Cosmic Rays.

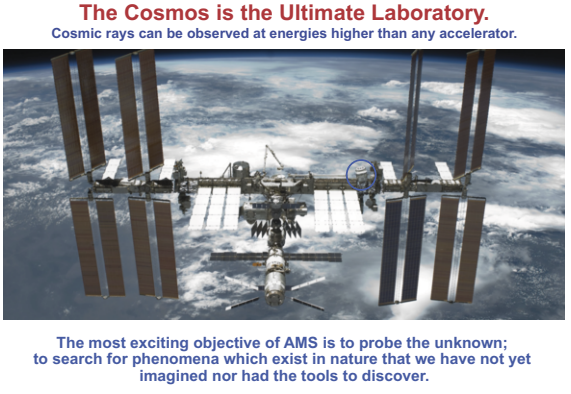

Figure 55: Among the physics objectives of AMS, the most exciting is to explore the unknown with a precision instrument.

Acknowledgments: AMS is an international collaboration sponsored by the U.S. DOE.
The full list of the AMS Collaboration Institutes and members is found on www.ams02.org/partners/participating-institutions/
We acknowledge the continuous strong support from DOE (J. Siegrist, M. Salamon). We also acknowledge the strong support of Mr. William Gerstenmaier, NASA Associate Administrator for Human Exploration and Operations, Mr. Trent Martin and Mr. Ken Bollweg, NASA Johnson Space Center (AMS Project Office). We also thank Professor Fernando Ferroni, President of INFN, Professor G. Bignami, President of INAF, Dr. Simona di Pippo, Head, European Space Policy Observatory who contributed to this Conference. The support of AS, ASI, CDTI, CERN, CSIST, DLR, INFN, MIT, and all our funding agencies is gratefully acknowledged.

References

[1] M. Turner and F. Wilczek, Phys. Rev. **D42** (1990) 1001; J. Ellis, 26th ICRC Salt Lake City (1999) astro-ph/9911440; H. Cheng, J. Feng and K. Matchev, Phys. Rev. Lett. **89** (2002) 211301; E. Ponton and L. Randall, JHEP **0904** (2009) 080; G. Kane, R. Lu and S. Watson, Phys. Lett. **B681** (2009) 151; Y–Z. Fan *et al.*, Int. J. Mod. Phys. **D19** (2010) 2011; M. Pato, M. Lattanzi and G. Bertone, JCAP **1012** (2010) 020.
[2] K. Luebelsmeyer *et al.*, Nucl. Instrum. Meth. **A 654** (2011) 639.
[3] M. Aguilar *et al.*, Phys. Rep. **366/6** (2002) 331.
[4] Th. Kirn, Nucl. Instrum. Meth. **A 706C** (2013) 43; Ph. Doetinchem *et al.*, Nucl. Instrum. Meth. **A 558** (2006) 526; F. Hauler *et al.*, IEEE Trans. Nucl. Sci. **51** (2004) 1365.
[5] A. Basili *et al.*, Nucl. Instrum. Meth. **A 707** (2012) 99; V. Bindi *et al.*, Nucl. Instrum. Meth. **A 623** (2010) 968.
[6] B. Alpat *et al.*, Nucl. Instrum. Meth. **A 613** (2010) 207.
[7] M. Aguilar-Benitez *et al.*, Nucl. Instrum. Meth. **A 614** (2010) 237; M. Aguilar-Benitez *et al.*, Proc. 30th ICRC (2007); P. Aguayo *et al.*, Nucl. Instrum. Meth. **A 560** (2006) 291; B. Baret *et al.*, Nucl. Instrum. Meth. **A 525** (2004) 126; J. Casaus, Nucl. Phys. B (Proc. Suppl.) **113** (2002) 147.
[8] C. Adloff *et al.*, Nucl. Instrum. Meth. (2013), 714 (2013), 147; F. Cadoux *et al.*, Nucl. Phys. B (Proc. Suppl.) **113** (2002) 159.